

Bridging the Gap Between Preference Alignment and Machine Unlearning

Xiaohua Feng¹ Yuyuan Li² Huwei Ji¹ Jiaming Zhang¹ Li Zhang¹ Tianyu Du¹ Chaochao Chen¹

Abstract

Despite advances in Preference Alignment (PA) for Large Language Models (LLMs), mainstream methods like Reinforcement Learning with Human Feedback (RLHF) face notable challenges. These approaches require high-quality datasets of positive preference examples, which are costly to obtain and computationally intensive due to training instability, limiting their use in low-resource scenarios. LLM unlearning technique presents a promising alternative, by directly removing the influence of negative examples. However, current research has primarily focused on empirical validation, lacking systematic quantitative analysis. To bridge this gap, we propose a framework to explore the relationship between PA and LLM unlearning. Specifically, we introduce a bi-level optimization-based method to quantify the impact of unlearning specific negative examples on PA performance. Our analysis reveals that not all negative examples contribute equally to alignment improvement when unlearned, and the effect varies significantly across examples. Building on this insight, we pose a crucial question: how can we optimally select and weight negative examples for unlearning to maximize PA performance? To answer this, we propose a framework called Unlearning to Align (U2A), which leverages bi-level optimization to efficiently select and unlearn examples for optimal PA performance. We validate the proposed method through extensive experiments, with results confirming its effectiveness.

1. Introduction

Despite the strong performance of Large Language Models (LLMs) in predicting the next token, their generated content often exhibits biases, factual inaccuracies, and other undesirable behaviors (Bai et al., 2022; Casper et al., 2023). Pref-

erence Alignment (PA) has been proposed to address these issues by guiding LLMs to generate responses aligned with human preferences, such as fairness and helpfulness (Christiano et al., 2017; Ziegler et al., 2019; Stiennon et al., 2020). This approach uses datasets of human-annotated preferred and non-preferred responses to optimize the model. Reinforcement Learning from Human Feedback (RLHF) is the primary method for achieving PA (Korbak et al., 2023; Wu et al., 2024; Azar et al., 2024), involving the training of a reward model on human preference data and optimizing the LLM using algorithms like Proximal Policy Optimization (PPO) (Schulman et al., 2017) or Direct Preference Optimization (DPO) (Rafailov et al., 2024). While RLHF shows strong performance across diverse applications, such as programming and creative writing, it relies on costly large-scale preference-aligned datasets, especially for positive examples (Yao et al., 2024). Additionally, RLHF training is computationally intensive and prone to instability (Liu et al., 2024b; Zhou et al., 2024), posing challenges for low-resource alignment scenarios.

As a key technique aimed at protecting user privacy, Machine Unlearning (MU) in LLMs offers a novel solution to the aforementioned challenges (Liu et al., 2024c; Yao et al., 2024). This technique enables the removal of specific user data from pre-trained LLMs without requiring a complete retraining of the model. By facilitating the unlearning of negative examples, this technique promotes PA while addressing the high costs and difficulties associated with acquiring positive examples for standard RLHF. Unlike RLHF, LLM unlearning requires only negative examples, which are typically easier and cheaper to collect via mechanisms like user reports or red team testing. For unaligned pre-trained models, identifying counterexamples can be highly automated, further reducing data collection costs. Additionally, the computational overhead of unlearning is comparable to fine-tuning and significantly lower than RLHF’s full training process, making it a practical approach for achieving alignment in low-resource scenarios.

Existing studies (Feng et al., 2024; Liu et al., 2024c; Yao et al., 2024) have validated the effectiveness of achieving model alignment through the unlearning of negative examples, highlighting the potential of integrating MU with PA. However, these studies primarily rely on experimental demonstrations, lacking in-depth quantitative analysis. For

¹Zhejiang University, Hangzhou, China ²Hangzhou Dianzi University, Hangzhou, China. Correspondence to: Chaochao Chen <zjuccc@zju.edu.cn>.

instance, the quantitative impact of unlearning specific samples on PA remains unclear. Additionally, critical questions such as which examples should be unlearned to maximize alignment and how to optimally select subsets of examples for unlearning to achieve the best outcomes remain unresolved. These gaps underscore a theoretical and practical disconnect between MU and PA. Addressing these challenges requires the development of a comprehensive analytical framework to unify these two domains and facilitate a deeper understanding of their intrinsic connections.

To address the identified challenges, we first develop a special bi-level optimization framework to quantify how unlearning specific negative samples impacts model PA performance. In particular, the inner optimization focuses on unlearning the target sample, while the outer optimization assesses the resulting change in PA performance. After further analysis, we find that not all negative examples contribute to PA improvement, with the degree of impact varying across examples. Meanwhile, the magnitude of the impact is influenced by the unlearning weights. This suggests that indiscriminately applying unlearning to all negative examples fails to achieve optimal PA performance. To address this, we propose a framework called Unlearning to Align (U2A), based on bi-level optimization, to strategically select samples and determine optimal unlearning weights. Further convergence and computational complexity analysis indicate that our proposed method demonstrates good applicability and efficiency in LLMs. This framework bridges the gap between MU and PA, offering a systematic approach to their integration. We summarize the main contributions of this paper as follows:

- We propose a special bi-level optimization framework to measure the impact of unlearning specific samples on PA performance, bridging the gap between MU and PA.
- We find that unlearning all negative examples does not always benefit PA, as their contributions to PA improvement vary and can be adjusted through unlearning weights.
- We propose the U2A framework, leveraging bi-level optimization to select and weight negative examples for unlearning, thereby maximizing PA performance.
- We conduct extensive evaluations on multiple models and real-world datasets, and the experimental results demonstrate the effectiveness of our method.

2. Related Work

2.1. Preference Alignment

PA methods can be broadly classified into learning-based and decoding-based methods, depending on whether model parameters are updated (Zhou et al., 2024). Learning-based methods (Ziegler et al., 2019; Stiennon et al., 2020;

Ouyang et al., 2022; Azar et al., 2024), such as RLHF, optimize models using preference datasets with techniques like PPO (Schulman et al., 2017), DPO (Rafailov et al., 2024), and Self-play Preference Optimization (SPO) (Wu et al., 2024). However, RLHF is computationally expensive (Rafailov et al., 2024). To mitigate this, decoding-based methods (Kim et al., 2023; Gao et al., 2023; Huang et al., 2024; Mudgal et al., 2024), which guide inference without parameter updates, have gained attention. Examples include rejection sampling (Mitchell et al., 2024; Beirami et al., 2024) and Monte Carlo Tree Search (Liu et al., 2023; Wan et al., 2024), which reduce computational costs by keeping parameters fixed. Since this study focuses on the relationship between MU and PA, and the former requires parameter updates, we primarily consider learning-based methods.

2.2. LLM unlearning

The goal of LLM unlearning is to remove specific knowledge from training data while preserving the model’s performance on unrelated tasks (Jang et al., 2023; Ji et al., 2024b; Liu et al., 2024a; Feng et al., 2024). Existing methods can be categorized into three main approaches: i) Gradient-based methods (Jang et al., 2023; Maini et al., 2024) use gradient ascent on the forget set (i.e., the data to be unlearned) to remove associated knowledge, with parameter regularization added to preserve performance on other tasks. ii) Preference optimization-based methods (Maini et al., 2024; Zhang et al., 2024) treat the forget set as negative examples or assign predefined responses (e.g., rejection responses) to achieve unlearning during PA. iii) Model weight-based methods (Jia et al., 2024b) analyze the roles of different model modules to guide unlearning, leveraging the modularity of LLMs. As model weight-based methods are primarily used for attribution analysis, this study focuses on gradient-based and preference optimization-based approaches.

3. Preliminary

Given a training set $\mathcal{D}_t = \{x^1, x^2, \dots, x^{N_t}\}$, where $x^i = \{x_1, x_2, \dots, x_{n_i}\}$ represents samples (i.e., sentences) with a token length of n_i , and N_t denotes the number of samples. A model π is trained on \mathcal{D}_t , and its optimal parameters θ^* satisfy the following equation:

$$\begin{aligned} \theta^* &= \arg \min_{\theta} \mathcal{L}_{\text{NLL}}(\mathcal{D}_t; \theta) \\ &= \arg \min_{\theta} -\mathbb{E}_{x^i \sim \mathcal{D}_t} \left[\sum_{t=1}^{n_i} \log p(x_t \mid x_{<t}; \theta) \right], \quad (1) \end{aligned}$$

where $p(x_t \mid x_{<t}; \theta) = \pi_{\theta}(x_t \mid x_{<t})$ denotes the prediction probability of model π_{θ} for the t -th token, given the first $t-1$ tokens as input. Next, we define the objectives for conducting RLHF and MU on the model π_{θ} , respectively.

3.1. Definition of RLHF

The standard RLHF paradigm consists of two main stages (Azar et al., 2024): i) learning a reward model, and ii) optimizing the policy (i.e., the model parameters) based on the learned reward.

In the reward model learning phase, a binary classifier is often trained using a logistic regression loss to distinguish preferred from non-preferred behaviors. A popular choice is the Bradley-Terry model (Bradley & Terry, 1952), where the pointwise reward $r(\mathbf{x}_{<t}, x_t)$ serves as the score for action x_t , given context $\mathbf{x}_{<t}$. Given a dataset $\mathcal{D}_a = \{\mathbf{x}_{<t}^i, x_t^i \succ \hat{x}_t^i\}_{i=1}^{N_a}$, where $x_t^i \succ \hat{x}_t^i$ denotes a preference for x_t^i over \hat{x}_t^i , the reward function is learned by minimizing the following logistic regression loss:

$$\mathcal{L}(r) = -\mathbb{E}_{(\mathbf{x}_{<t}^i, x_t^i \succ \hat{x}_t^i) \sim \mathcal{D}_a} [\log(p(x_t^i \succ \hat{x}_t^i | \mathbf{x}_{<t}^i))], \quad (2)$$

where $p(x_t^i \succ \hat{x}_t^i | \mathbf{x}_{<t}^i) = \sigma(r(\mathbf{x}_{<t}^i, x_t^i) - r(\mathbf{x}_{<t}^i, \hat{x}_t^i))$ and $\sigma(\cdot)$ denotes the sigmoid function.

Based on the reward function, the objective of RLHF is to maximize the expected reward while minimizing the divergence between the policy π_θ and a reference policy π_{ref} . The specific objective can be expressed as:

$$\mathcal{J}(\theta) = \mathbb{E}_{\pi_\theta}[r(\mathbf{x}_{<t}^i, x_t^i)] - \tau D_{\text{KL}}(\pi_\theta \parallel \pi_{\text{ref}}), \quad (3)$$

where $\mathbf{x}_{<t}^i \sim \rho$ denote the sampled history, $x_t^i \sim \pi_\theta(\cdot | \mathbf{x}_{<t}^i)$ denote the action drawn from the policy, and τ is the parameter balancing the alignment and regularization objectives. The KL divergence D_{KL} is used to quantify the difference between the reference and current policies. Since LLM unlearning in this work incorporates a regularization term with analogous effects, we retain only the reward term in Eq. (3).

3.2. Definition of LLM Unlearning

Mainstream methods for unlearning in LLMs typically involve fine-tuning the original model with an unlearning objective function. Given a forget set \mathcal{D}_f , while specific designs vary, the loss function in LLM unlearning tasks can generally be expressed as:

$$\mathcal{L}(\theta) = \mathcal{L}_{\text{forget}}(\mathcal{D}_f; \theta) + \lambda \mathcal{L}_{\text{reg}}(\theta). \quad (4)$$

Here, $\mathcal{L}_{\text{forget}}$ often is a loss term targeting data to be unlearned, reducing the model’s performance on these samples to minimize their influence on future predictions. To preserve the model’s overall performance on unrelated data and confine unlearning to the intended scope, regularization terms \mathcal{L}_{reg} such as output loss or divergence regularization are commonly introduced. These terms essentially act as parameter regularization. Specifically, commonly used loss-based methods (Jia et al., 2024a; Ji et al., 2024b) typically integrate one or more of the loss components. For readability, in this paper, we employ the widely adopted gradient

ascent unlearning loss and parameter regularization loss as general objectives for LLM unlearning, considering their broad applicability. The formalization is as follows:

$$\min_{\theta} \underbrace{\frac{1}{|\mathcal{D}_f|} \sum_{i=1}^{|\mathcal{D}_f|} \sum_{t=1}^{n_i} \log p(x_t^i | \mathbf{x}_{<t}^i; \theta)}_{\mathcal{L}_{\text{forget}}(\mathcal{D}_f; \theta)} + \lambda \underbrace{\|\theta - \theta^*\|^2}_{\mathcal{L}_{\text{reg}}(\theta)}. \quad (5)$$

A more detailed discussion on the definition of LLM unlearning can be found in Appendix A.

4. Connection between MU and PA

4.1. Impact of MU on PA

Given a training sample \mathbf{x} to be unlearned, the unlearning objective in an LLM is described by Eq (5). We adopt a special bi-level optimization framework to link MU with PA, quantifying how unlearning a single sample affects the model’s PA performance. In this setup, the inner problem ensures the unlearning objective is achieved, while the outer problem evaluates its impact on PA performance. Specifically, we assume that the degree of unlearning for a sample \mathbf{x} is represented by the weight $\omega \geq 0$, and the model parameters that satisfy the unlearning objective under this condition are denoted as $\theta^*(\omega)$. The bi-level optimization problem is formulated as:

$$\begin{aligned} &\text{Find } \mathcal{J}(\theta^*(\omega)) - \mathcal{J}(\theta^*(0)) \\ &\text{s.t. } \theta^*(\omega) = \arg \min_{\theta} \omega \mathcal{L}_{\text{forget}}(\mathbf{x}; \theta) + \lambda \mathcal{L}_{\text{reg}}(\theta), \end{aligned} \quad (6)$$

where $\mathcal{J}(\theta^*(\omega))$ represents the PA performance of the model when the unlearning weight is ω . For example, $\mathcal{J}(\theta^*(0))$ represents the PA performance of the model without any unlearning. Inspired by the implicit function method for solving bi-level optimization problems, we further derive and prove Proposition 4.2.

Assumption 4.1. $\mathcal{L}_{\text{forget}}(\mathbf{x}; \theta)$ is continuously differentiable w.r.t. θ , and its Hessian matrix is positive semidefinite. $\mathcal{J}(\theta)$ is twice continuously differentiable w.r.t. θ .

Proposition 4.2. *If Assumptions 4.1 holds, the change in PA performance for a model with parameters θ^* after unlearning sample \mathbf{x} using unlearning weight ω satisfies:*

$$\Delta \mathcal{J}(\theta^*(\omega)) \approx -\frac{\omega}{2} \nabla_{\theta} \mathcal{J}(\theta^*)^{\top} \nabla_{\theta} \mathcal{L}_{\text{forget}}(\mathbf{x}; \theta^*). \quad (7)$$

Proof. The proof can be found in Appendix B.1. \square

According to Proposition 4.2, we can directly set the unlearning weight ω to 1 (i.e., $\Delta \mathcal{J}(\theta^*(1))$) to quantitatively assess the impact of unlearning a single sample on the model’s

PA performance. To further analyze the factors influencing $\Delta\mathcal{J}(\theta^*(\omega))$, we decompose the gradient inner product into the gradient norm and the cosine of the angle between gradients, as follows:

$$\Delta\mathcal{J}(\theta^*(\omega)) \approx -\frac{\omega}{2} \|\nabla_{\theta}\mathcal{J}(\theta^*)\| \cdot \|\nabla_{\theta}\mathcal{L}_{\text{forget}}(\mathbf{x}; \theta^*)\| \cdot \cos(\phi), \quad (8)$$

where $\cos(\phi)$ denotes the angle between the two gradient vectors. Then, the following conclusions can be drawn:

- **Conclusion 1: impact can be positive or negative.** The impact of unlearning a sample on PA performance can be either positive or negative, depending on the gradient direction relationship (i.e., the sign of $\cos(\phi)$), which is partially influenced by the reward of the unlearned sample's combination. A sample \mathbf{x} can be represented as multiple combinations, i.e., $\mathbf{x} = \{\mathbf{x}_{<t}, \mathbf{x}_t\}_{t=1}^n$. For low-reward combinations, where generated behavior often deviates significantly from human preferences, the unlearning objective gradient direction (i.e., the direction increasing the sample's generation probability) is more likely to oppose the PA objective gradient direction. This results in $\cos(\phi) < 0$ and $\Delta\mathcal{J}(\theta^*(\omega)) > 0$. Further analysis indicates that if the rewards for most combinations $\{\mathbf{x}_{<t}, \mathbf{x}_t\}$ in a sample \mathbf{x} are low, unlearning the sample tends to improve preference alignment. Conversely, if only a few combinations have low rewards, unlearning the sample will likely hinder PA.
- **Conclusion 2: magnitude of impact varies.** The effect of unlearning on PA performance varies across samples and is influenced by the unlearning degree and gradient norm. The gradient norm is an inherent property of the sample, such as the model's degree of fit to the sample. For samples that the model fits well, the gradient norm tends to be smaller. On the other hand, the unlearning weight is a controllable factor that can be adjusted by tuning parameters such as the unlearning weight.

4.2. A Weighted MU Framework for PA

The above conclusions indicate that, given a set $\mathcal{D} = \{\mathbf{x}^i\}_{i=1}^n$ containing n negative samples, simply performing the unlearning operation directly according to Eq. (5) does not guarantee optimal PA results. This is primarily due to the following two issues:

- **Issue 1.** Conclusion 1 suggests that for a given negative sample \mathbf{x}^i , which contains some low-reward combinations, this alone does not imply that unlearning \mathbf{x}^i will necessarily promote PA. The effectiveness of unlearning also depends on the proportion of low-reward components within the sample. This indicates that not all negative samples need to be unlearned.

- **Issue 2.** Conclusion 2 indicates that even if different negative samples (e.g., \mathbf{x}^i and \mathbf{x}^j) can both promote PA, the degree of promotion may vary. This difference can be controlled by adjusting the unlearning weight ω .

Problem setup. To address these two issues, we propose a framework called Unlearning to Align (U2A) based on a sample-weighting approach. This framework achieves the maximization of PA performance by assigning higher weights to samples that contribute more significantly to performance improvement during the unlearning process. Specifically, when the weight ω is set to 0, it indicates that the corresponding sample is not selected for unlearning. For ease of analysis and discussion, we assume that the weight vector $\omega = [\omega_1, \omega_2, \dots, \omega_n]$ lies on an n -dimensional simplex, and we denote the unlearning loss of each sample \mathbf{x}^i as $\ell_i(\theta)$. The U2A framework can be formalized as solving the following optimization problem:

$$\begin{aligned} \min_{\omega \in \Delta_n} \quad & -\mathcal{J}(\theta^*(\omega)) + \beta L_p(\omega) \\ \text{s.t.} \quad & \theta^*(\omega) = \arg \min_{\theta} \sum_{i=1}^n \omega_i \ell_i(\theta) + \lambda \mathcal{L}_{\text{reg}}(\theta), \end{aligned} \quad (9)$$

where $L_p(\omega)$ represents an introduced L_p -norm sparsity-inducing regularization term to ensure that the number of selected samples for unlearning is as small as possible, and β denotes the weight coefficient of the regularization term. Further analysis shows that when $p = 1$, the sparsity regularization has relatively weak compressive effects on small values. On the other hand, when $p = 0$, it can effectively control the sparsity of weights (i.e., the number of non-zero weights). However, in this case, the regularization term $L_q(\omega)$ becomes a non-continuous and non-convex function, which significantly increases the difficulty of optimization. Considering these factors, when $p = \frac{1}{2}$, the regularization term $L_p(\omega)$ is both a strictly convex function and exhibits good smoothness. Therefore, in this paper, we set $p = \frac{1}{2}$, making $L_p(\omega) = \sum_{i=1}^n \sqrt{\omega_i}$. Solving Eq. (9) yields the selected unlearning set \mathcal{S} as well as the unlearning weight ω for each sample.

U2A framework. To enhance clarity, we denote the outer objective function as $g(\omega)$ and the inner objective function as $f(\theta, \omega)$. If $f(\theta, \omega)$ is twice differentiable w.r.t. θ , the constraint $\theta^*(\omega) = \arg \min_{\theta} f(\theta, \omega)$ can be relaxed into $\frac{\partial f(\theta, \omega)}{\partial \theta} \big|_{\theta=\theta^*(\omega)} = 0$. When $f(\theta, \omega)$ is strictly convex w.r.t. θ , this relaxation becomes tight (Borsos et al., 2024). Assumption 4.1 ensures this property, enabling the use of first-order optimization methods (Pedregosa, 2016; Finn et al., 2017; Liu et al., 2019) to solve Eq. (6) and avoiding computationally expensive naive greedy algorithms. Considering the computation efficiency, we adopt a variant of the cone-constrained generalized matching pursuit algorithm (Lo-

Algorithm 1 U2A Algorithm

- 1: **Input:** Dataset $\mathcal{D} = \{x^i\}_{i=1}^n$, initial model parameter θ^* , maximum number of iterations T , early stopping threshold δ , regularization coefficient λ and β .
- 2: **Output:** unlearning set $\mathcal{S}^{\text{final}}$ and weights $\omega^{\text{final},*}$.
- 3: **Initialization:** Initialize weights $\omega^{1,*} = [0, \dots, 0]$, randomly select one point to initialize the unlearning set $\mathcal{S}^1 = \{i\}$, and set $\omega_i^{1,*} = 1$.
- 4: **for** $t = 2$ to T **do**
- 5: Gradient descent to solve the inner problem of Eq. (9) to obtain $\theta^*(\omega^{t-1,*})$.
- 6: Fix current model parameter $\theta^*(\omega^{t-1,*})$, and optimize the weights $\omega^{t,*}$ according to Eq. (10).
- 7: Select point k^* with the maximum $\Delta g(k)$ using Eq. (12).
- 8: Update the unlearning set $\mathcal{S}^t = \mathcal{S}^{t-1} \cup \{k^*\}$ and set $\omega_k^{t,*} = 1$.
- 9: **if** $g(\omega^{t-1,*}) - g(\omega^{t,*}) \leq \delta$ **then**
- 10: **Break.**
- 11: **end if**
- 12: **end for**
- 13: Re-optimize the weights $\omega^{\text{final},*}$ on the final unlearning set $\mathcal{S}^{\text{final}}$.

catello et al., 2017), which performs incremental optimization. This approach iteratively constructs the unlearning set \mathcal{S} , thereby significantly reducing computational complexity.

Specifically, in each iteration, we first solve the inner optimization problem using the gradient descent method to obtain the model parameters $\theta^*(\omega)$ with optimal unlearning performance. Subsequently, we fix the model parameters to solve the outer optimization problem to obtain the solution $\omega^{t,*}$, which can be formalized as:

$$\omega^{t,*} = \arg \min_{\omega \in \Delta_n} g(\omega) \quad \text{s.t.} \quad \text{supp}(\omega) = \mathcal{S}_{t-1}, \quad (10)$$

where the constraint is imposed to restrict the support set of the weight vector ω to be identical to the current unlearning set \mathcal{S}_{t-1} . In other words, the non-zero components of ω are confined to elements within the current unlearning set, thereby preventing the introduction of new sample points. It is important to note that the support set $\text{supp}(\omega) = \{i \mid \omega_i \neq 0\}$ represents the index set of the non-zero elements in ω . This can be solved by using the projected gradient descent method. According to the implicit function theorem, the gradient of $g(\omega)$ w.r.t. ω can be expressed as:

$$\nabla_{\omega} g(\omega) = \nabla_{\theta} \mathcal{J}(\theta^*(\omega)) \left(\frac{\partial^2 f}{\partial \theta^2} \right)^{-1} \sum_{i=1}^n \nabla_{\theta} \ell_i(\theta^*(\omega)) + \frac{\beta}{2} \omega^{-\frac{1}{2}}, \quad (11)$$

where $\frac{\partial^2 f}{\partial \theta^2} = \sum_{i=1}^n \omega_i \nabla_{\theta}^2 \ell_i(\theta^*(\omega)) + 2\lambda I$, denoting the Hessian matrix of the inner optimization problem (details are provided in Appendix B.2). Given that explicitly com-

puting the inverse of the Hessian matrix is computationally prohibitive in LLM applications, directly solving the problem is impractical. Therefore, we adopt the conjugate gradient method (Nocedal & Wright, 2006), which iteratively computes the product of the Hessian matrix and gradient vector, thereby reducing the computational complexity.

After completing the outer optimization, we identify a new sample point k to add to the unlearning set based on the marginal gain of the outer objective function $g(\omega)$, with the goal of maximizing the marginal gain. The marginal gain is calculated as $\Delta g(k) = \frac{\partial g(\omega)}{\partial \omega_k}$. According to Eq. (11), its expression can be derived as follows:

$$\Delta g(k) = \nabla_{\theta} \mathcal{J}(\theta^*(\omega)) \left(\frac{\partial^2 f}{\partial \theta^2} \right)^{-1} \nabla_{\theta} \ell_k(\theta^*(\omega)) + \frac{\beta}{2} \omega_k^{-\frac{1}{2}}. \quad (12)$$

After computing the marginal gain, we select the sample point with the maximum gain $k^* = \arg \max_{k \in [1, n]} \Delta g(k)$, add it to the unlearning set \mathcal{S}_{t-1} . The detailed implementation of the algorithm is provided in Algorithm 1.

Convergence analysis. Lemma 4.3 indicates that as the number of iterations t increases, the solution obtained by our U2A algorithm gradually approaches the optimal solution, and the error decreases at $\mathcal{O}(1/t)$. Theorem 4.4 demonstrates that as the size of the unlearning set m increases, the approximation error gradually diminishes. This implies that it is unnecessary to unlearn all negative examples, selecting a subset is sufficient to make the value of the objective function very close to the optimal value of the original problem.

Lemma 4.3. Suboptimality Bound (cf. Theorem 2 of Locatello et al. (2017)). Assume $g(\omega)$ is L -smooth, and let the initial suboptimality be denoted as $\varepsilon_1 = g(\omega^{1,*}) - g(\omega^*)$. After t iterations, the suboptimality bound of the U2A algorithm can be expressed as:

$$g(\omega^{t,*}) - g(\omega^*) \leq \frac{8L + 4\varepsilon_1}{t + 3},$$

where $g(\omega^*)$ represents the global optimal value. In the case of a non-convex objective function, $g(\omega^*)$ is approximated as a certain local optimal value.

Theorem 4.4. Size of Unlearning Set. Under the condition that the suboptimality error does not exceed ε , the size m of the final unlearning set satisfies:

$$m \in \mathcal{O}((L + \varepsilon_1)\varepsilon^{-1}).$$

That is, the size of the final unlearning set is proportional to the smoothness of the objective function and the initial suboptimality ε_1 , while being inversely proportional to the target precision ε .

Proof. The proof can be found in Appendix B.3. \square

Complexity analysis. The inner optimization problem must be solved in each iteration to determine the optimal model parameter. Assuming t_f gradient descent iterations are required, with each iteration computing gradients for all data points, and the gradient computation complexity for a single data point is c , the total complexity of the inner optimization is $\mathcal{O}(t_f \cdot n \cdot c)$. For the outer problem, given an unlearning set \mathcal{S}^t with t samples, and t_ω updates required per optimization, the complexity of solving $\omega^{t,*}$ is $\mathcal{O}(t \cdot t_\omega \cdot d)$, where d is the model parameter dimension. Marginal gain computation involves implicit gradient calculations. Using the conjugate gradient method with t_g iterations, where each iteration requires a Hessian-vector product computation of complexity $\mathcal{O}(t_g \cdot n \cdot c)$, and computing the gradients of all data points w.r.t. θ contributes an additional complexity of $\mathcal{O}(n \cdot c)$. Thus, the total complexity for marginal gain computation is $\mathcal{O}((t_g + 1) \cdot n \cdot c)$. Finally, if the final unlearning set contains m samples, the overall algorithm complexity can be expressed as:

$$\mathcal{O}(m \cdot ((t_f + t_g + 1) \cdot n \cdot c + n \cdot d + m \cdot t_\omega \cdot d)).$$

This demonstrates that our U2A algorithm is computationally efficient and well-suited for high-dimensional applications, such as LLMs.

5. Experiment

5.1. Experiment Setups

Datasets. In our experiments, we evaluate across three mainstream PA tasks and datasets: (i) reducing harmfulness **PKU SafeRLHF** (Dai et al., 2023), (ii) enhancing usefulness **UltraFeedback** (Cui et al., 2023; Tunstall et al., 2023), (iii) eliminating hallucinations **HaluEval** (Li et al., 2023). For each dataset, we randomly sample 80% of the examples to construct the fine-tuning set \mathcal{D}_{FIN} , while the remaining examples \mathcal{D}_{PA} are reserved for evaluating the model’s PA performance post-unlearning. From \mathcal{D}_{FIN} , we further extract 12.5% negative samples to construct a subset \mathcal{D}_{SEL} , representing selectively forgettable negative examples. Details of this partitioning are provided in Appendix C.1.

Base and preference reward models. Following the configurations in prior study (Jia et al., 2024a; Zhou et al., 2024), we select the widely used Llama-2-7B-Chat (Touvron et al., 2023) and Llama-3.1-8B-Instruct (Dubey et al., 2024) as base models for each dataset. The base models are first fine-tuned on \mathcal{D}_{FIN} to obtain the original models requiring unlearning. Additionally, we fine-tune the base models on \mathcal{D}_{FIN} excluding the negative samples \mathcal{D}_{SEL} . For PA evaluation, we employ the Beaver-7B-v3.0-Reward model (Dai et al., 2023; Ji et al., 2024a).

Evaluation metrics. We evaluate our proposed method along two dimensions: PA performance and unlearning performance. For PA performance, in the PKU SafeRLHF dataset, we utilize two metrics, Reward-value (Chakraborty et al., 2024; Yao et al., 2024) and ASR (Xu et al., 2024), where ASR can be further divided into four dimensions: ASR-keyword, ASR-answer, ASR-useful, and ASR-summary. In the UltraFeedback Binarized dataset, we evaluate PA performance using Win-rate (Xiao et al., 2024; Rafailov et al., 2024) and Coherence (Chakraborty et al., 2024; Khanov et al., 2024; Kong et al., 2024), where the Win-rate includes Length-control Win Rate and Win Rate vs. GPT-4. In the HaluEval dataset, Hallucination-rate (Yao et al., 2024) is adopted as the evaluation metric, including F1, Precision and Recall. For unlearning performance, we evaluate unlearning effectiveness and model utility. Unlearning effectiveness for PKU SafeRLHF, UltraFeedback and HaluEval is measured using Membership Inference Attack (MIA) (Jia et al., 2024a). Model utility is evaluated with Perplexity (PPL) (Yao et al., 2024; Doshi & Stickland, 2024). Details are provided in Appendix C.2.

Baselines. We evaluate our proposed method U2A against widely acknowledged baselines, including unlearning methods (i.e., Retrain, GA (Maini et al., 2024), GradDiff (Liu et al., 2022; Yao et al., 2024), and NPO (Zhang et al., 2024)), as well as PA methods (i.e., PPO (Schulman et al., 2017) and DPO (Rafailov et al., 2024)). The effectiveness of our method is validated by comparing the U2A-improved unlearning baseline with the original baseline and existing PA baselines.

Training setup. We use the AdamW (Loshchilov, 2017) optimizer with a learning rate of $4e - 6$ for training, and a learning rate of $3e - 2$ for updating the unlearning weights. Both optimizers utilize a cosine annealing scheduler for learning rate scheduling. The hyperparameters of baselines are kept as reported in their original papers. For our method, the regularization coefficient is set to $\lambda = 1.0$, the scaling coefficient to $\beta = 0.5$, the early stopping threshold δ to 0.01, and the maximum iterations to 100. All experiments were conducted on NVIDIA A800 GPUs. For the PKU SafeRLHF dataset and the HaluEval dataset, the number of iterations was set to 50, with the number of update epochs set to 5. For the UltraFeedback Binarized dataset, the number of iterations was set to 25, with the number of update epochs set to 10.

5.2. Experiment Results

Unlearning affects PA. We assess the impact of unlearning individual samples on PA performance using the Llama-2-7B-Chat model across three datasets. Given the nearly negligible effect of unlearning a single sample on model

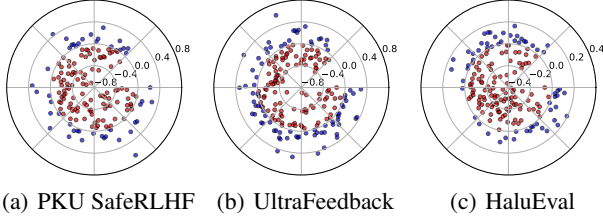


Figure 1. Effect of unlearning individual data samples on PA performance of Llama-2-7B-Chat model. Each point represents PA performance change after unlearning a specific data sample. The angle of each point follows a uniform distribution, while the radial distance indicates the magnitude of PA performance change. Red points represent negative effects (i.e., unlearning this sample led to worse PA), whereas blue points represent positive effects (i.e., unlearning this sample improved PA). Note that larger distances from the origin correspond to stronger impacts on PA performance.

parameters, we randomly select 150 groups, each with 32 negative samples, from a pool of eligible negative samples. PA performance changes after unlearning each group are compared, with parameter ω set to 1. Figure 1 shows that unlearning can have both positive and negative effects, suggesting that removing negative samples does not consistently improve PA performance. Additionally, the degree of improvement varies significantly across different samples.

To better understand this, we decompose reward values for each token. Tokens with reward values below the average reward across all tokens are classified as “low-reward”, while those above the average are categorized as “high-reward”. The average reward values for each dataset are as follows: -1.7463 for PKU SafeRLHF, 0.9001 for UltraFeedback, and -0.7839 for HaluEval. To distinguish the impact of different sample groups, we apply a threshold on the proportion of low-reward tokens. Specifically, samples with a low-reward token proportion below the threshold (0.60 for PKU SafeRLHF, 0.575 for UltraFeedback, and 0.575 for HaluEval) are marked in red, while those exceeding the threshold are marked in blue. Figure 2 illustrates the impact of unlearning these samples on PA performance. Taking the PKU SafeRLHF dataset as an example, when the proportion of low-reward tokens in the unlearned dataset exceeds the threshold (dashed vertical line at 0.6), most changes value of PA performance are positive, indicating an improvement in PA. Conversely, when the proportion of low-reward tokens is below the threshold, most changes value of PA performance are negative, suggesting that unlearning such samples tends to degrade PA performance. Overall, red samples, with more dispersed rewards and fewer low-reward tokens, tend to hinder PA performance improvement when unlearned. In contrast, unlearning blue samples, characterized by a higher proportion of low-reward tokens, significantly boost PA performance. These findings align with our theoretical analysis

in Section 4.1.

Effectiveness of U2A. To validate the effectiveness of our proposed U2A framework, we conduct experiments using the Llama-2-7B-Chat and Llama-3.1-8B-Instruct models on three datasets. We first apply existing unlearning baseline methods to all eligible negative samples. Next, we integrate the U2A framework with these baselines using a sample-weighted unlearning approach. Finally, we employ existing PA baselines to perform direct PA on subsets of the alignment datasets \mathcal{D}_{PA} . We report the comparison of PA and unlearning performance across different methods in Table 1. The results show that improving unlearning baselines with the U2A framework yields significant PA performance improvements, while maintaining comparable unlearning performance. Additionally, the improved unlearning methods outperform PA baselines in PA performance to a certain extent. These results highlight the potential of leveraging unlearning mechanisms to enhance alignment, further validating the effectiveness of our proposed method. Results for other tasks are reported in Appendix D.

Efficiency of U2A. We assess the efficiency of the U2A-improved unlearning baseline against existing PA methods on the PKU SafeRLHF dataset using the Llama-2-7B-Chat model. With identical hyperparameters and early stopping conditions (training halts when the PA score surpasses 0.745), we compare the number of update iterations and per-iteration time costs. Table 2 summarizes the results, showing that the U2A-enhanced method significantly reduces update iterations needed to reach the target PA score. Moreover, although it introduces additional computation, leading to an increase in the average per-iteration time, the significant reduction in the number of iterations results in a training time reduction of approximately 90% compared to PA baselines such as PPO and DPO. These findings confirm the U2A framework’s efficiency and practicality under resource-limited settings.

6. Conclusion

The mainstream PA approach, RLHF, faces significant challenges in low-resource settings, including (1) reliance on numerous positive preference samples, which are costly to obtain, and (2) instability during training, resulting in high computational and management costs. To address these issues, we propose a MU-based method that reduces dependence on positive samples by mitigating the influence of negative samples to achieve PA. Our method achieves computational efficiency comparable to standard fine-tuning while showing strong potential. We first develop a bi-level optimization framework to evaluate the impact of unlearning individual samples on PA performance. Through this analysis, we observe that negative samples contribute un-

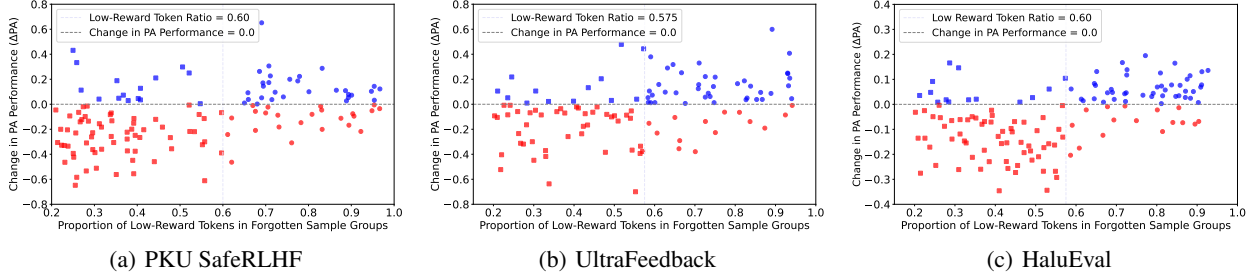


Figure 2. Analysis of how unlearning data samples affects PA performance. Each point represents the change in PA performance (Δ PA) after unlearning a group of samples. The x -axis denotes the proportion of low-reward tokens in the unlearned sample groups, and the y -axis represents the corresponding change in PA performance. Points are colored based on Δ PA: blue indicates a positive change, while red indicates a negative change. The shapes further differentiate the groups: squares represent sample groups with a low proportion of low-reward tokens (i.e., high-reward samples), whereas circles represent sample groups with a high proportion of low-reward tokens (i.e., low-reward samples).

Table 1. Comparison of the U2A framework with the current PA and unlearning baseline methods on the PKU SafeRLHF dataset. For the same baseline before and after improvement, consistent experimental settings are ensured. Optimal results are highlighted in **bold**.

Models	Methods	PA Performance					MU Performance	
		Reward-value (\uparrow)	ASR-keyword (\downarrow)	ASR-answer (\downarrow)	ASR-useful (\downarrow)	ASR-summary (\downarrow)	MIA (\uparrow)	PPL (\downarrow)
Llama-2-7B-Chat	Original	-5.84	78.65	54.42	30.19	61.54	0.4892	76.49
	Retrain	-4.23	73.08	62.69	24.23	59.42	0.4866	104.36
	PPO	-0.59	74.42	58.65	29.62	52.50	0.4884	103.39
	DPO	-2.30	72.27	56.15	27.31	52.69	0.4892	76.28
	GA	-4.58	84.04	56.92	29.23	54.42	0.4862	71.46
	GradDiff	-4.76	82.35	58.17	25.40	56.95	0.4912	60.11
	NPO	-5.96	77.69	54.30	30.05	68.82	0.4891	76.50
	GA + U2A	1.49	74.13	53.19	21.19	48.74	0.4770	56.31
	GradDiff + U2A	2.63	73.46	57.00	24.75	50.20	0.4992	51.28
	NPO + U2A	-3.65	77.12	52.51	23.65	56.26	0.4892	67.74
Llama-3.1-8B-Instruct	Original	-3.82	99.23	91.73	13.65	90.19	0.4946	2.01
	Retrain	-2.11	99.81	90.58	14.04	87.69	0.4963	2.07
	PPO	-1.07	96.73	83.65	10.19	79.81	0.4881	2.01
	DPO	-1.33	95.33	79.01	11.77	82.59	0.4919	2.08
	GA	-2.56	96.17	75.11	11.45	70.33	0.4978	2.03
	GradDiff	-1.87	85.34	63.55	15.97	52.55	0.5127	2.06
	NPO	-3.77	98.65	91.57	13.90	90.37	0.3924	2.11
	GA + U2A	0.03	92.31	71.35	10.15	62.48	0.5563	2.01
	GradDiff + U2A	0.95	83.63	62.28	9.65	49.50	0.5489	1.96
	NPO + U2A	-0.21	96.68	89.74	11.62	88.56	0.4723	2.05

Table 2. Comparison of the efficiency of different methods. We set an early stopping condition, where PA reaches a fixed value 0.745, and compare the number of epochs (update rounds) and the time costs of different methods. The experimental setups remain consistent before and after the improvement using U2A. Optimal results are highlighted in **bold**.

Methods	Update Rounds	Time Costs(s)	Methods	Update Rounds	Time Costs(s)	Methods	Update Rounds	Time Costs(s)
Retrain	197	241.2498	GA	142	167.1139	GA + U2A	46	248.3760
PPO	282	911.7341	GradDiff	764	995.9192	GradDiff + U2A	19	70.8349
DPO	1353	3619.9515	NPO	751	967.1019	NPO + U2A	29	132.1398

evenly to PA, with many offering limited benefits. This observation leads to a key question: how can we selectively weight and unlearn negative samples to optimize alignment? To this end, we formally define the problem and introduce U2A, a framework leveraging bi-level optimization to efficiently select and weighted unlearn samples for improved

alignment. Experiments demonstrate that U2A significantly enhances alignment efficiency and effectiveness, underscoring its value in resource-constrained scenarios. By linking PA with MU, this work provides a novel perspective on PA for LLMs and suggests new directions for optimizing PA algorithms.

References

- Azar, M. G., Guo, Z. D., Piot, B., Munos, R., Rowland, M., Valko, M., and Calandriello, D. A general theoretical paradigm to understand learning from human preferences. In *International Conference on Artificial Intelligence and Statistics*, pp. 4447–4455. PMLR, 2024.
- Bai, Y., Jones, A., Ndousse, K., Askell, A., Chen, A., Das-Sarma, N., Drain, D., Fort, S., Ganguli, D., Henighan, T., et al. Training a helpful and harmless assistant with reinforcement learning from human feedback. *arXiv preprint arXiv:2204.05862*, 2022.
- Beirami, A., Agarwal, A., Berant, J., D’Amour, A., Eisenstein, J., Nagpal, C., and Suresh, A. T. Theoretical guarantees on the best-of-n alignment policy. *arXiv preprint arXiv:2401.01879*, 2024.
- Borsos, Z., Mutn , M., Tagliasacchi, M., and Krause, A. Data summarization via bilevel optimization. *Journal of Machine Learning Research*, 25(73):1–53, 2024.
- Bradley, R. A. and Terry, M. E. Rank analysis of incomplete block designs: I. the method of paired comparisons. *Biometrika*, 39(3/4):324–345, 1952.
- Casper, S., Davies, X., Shi, C., Gilbert, T. K., Scheurer, J., Rando, J., Freedman, R., Korbak, T., Lindner, D., Freire, P., et al. Open problems and fundamental limitations of reinforcement learning from human feedback. *arXiv preprint arXiv:2307.15217*, 2023.
- Chakraborty, S., Ghosal, S. S., Yin, M., Manocha, D., Wang, M., Bedi, A. S., and Huang, F. Transfer q star: Principled decoding for llm alignment. *arXiv preprint arXiv:2405.20495*, 2024.
- Christiano, P. F., Leike, J., Brown, T., Martic, M., Legg, S., and Amodei, D. Deep reinforcement learning from human preferences. *Advances in neural information processing systems*, 30, 2017.
- Cui, G., Yuan, L., Ding, N., Yao, G., Zhu, W., Ni, Y., Xie, G., Liu, Z., and Sun, M. Ultrafeedback: Boosting language models with high-quality feedback. 2023.
- Dai, J., Pan, X., Sun, R., Ji, J., Xu, X., Liu, M., Wang, Y., and Yang, Y. Safe rlhf: Safe reinforcement learning from human feedback. *arXiv preprint arXiv:2310.12773*, 2023.
- Dige, O., Arneja, D., Yau, T. F., Zhang, Q., Bolandraftar, M., Zhu, X., and Khattak, F. Can machine unlearning reduce social bias in language models? In *Proceedings of the 2024 Conference on Empirical Methods in Natural Language Processing: Industry Track*, pp. 954–969, 2024.
- Doshi, J. and Stickland, A. C. Does unlearning truly unlearn? a black box evaluation of llm unlearning methods. *arXiv preprint arXiv:2411.12103*, 2024.
- Dubey, A., Jauhri, A., Pandey, A., Kadian, A., Al-Dahle, A., Letman, A., Mathur, A., Schelten, A., Yang, A., Fan, A., et al. The llama 3 herd of models. *arXiv preprint arXiv:2407.21783*, 2024.
- Fan, C., Liu, J., Lin, L., Jia, J., Zhang, R., Mei, S., and Liu, S. Simplicity prevails: Rethinking negative preference optimization for llm unlearning. *arXiv preprint arXiv:2410.07163*, 2024.
- Feng, X., Chen, C., Li, Y., and Lin, Z. Fine-grained plugable gradient ascent for knowledge unlearning in language models. In *Proceedings of the 2024 Conference on Empirical Methods in Natural Language Processing*, pp. 10141–10155, 2024.
- Finn, C., Abbeel, P., and Levine, S. Model-agnostic meta-learning for fast adaptation of deep networks. In *International conference on machine learning*, pp. 1126–1135. PMLR, 2017.
- Gao, L., Schulman, J., and Hilton, J. Scaling laws for reward model overoptimization. In *International Conference on Machine Learning*, pp. 10835–10866. PMLR, 2023.
- Huang, J. Y., Sengupta, S., Bonadiman, D., Lai, Y.-a., Gupta, A., Pappas, N., Mansour, S., Kirchhoff, K., and Roth, D. Deal: Decoding-time alignment for large language models. *arXiv preprint arXiv:2402.06147*, 2024.
- Jang, J., Yoon, D., Yang, S., Cha, S., Lee, M., Logeswaran, L., and Seo, M. Knowledge unlearning for mitigating privacy risks in language models. In *Proceedings of the 61st Annual Meeting of the Association for Computational Linguistics (Volume 1: Long Papers)*, pp. 14389–14408, 2023.
- Ji, J., Liu, M., Dai, J., Pan, X., Zhang, C., Bian, C., Chen, B., Sun, R., Wang, Y., and Yang, Y. Beavertails: Towards improved safety alignment of llm via a human-preference dataset. *Advances in Neural Information Processing Systems*, 36, 2024a.
- Ji, J., Liu, Y., Zhang, Y., Liu, G., Kompella, R. R., Liu, S., and Chang, S. Reversing the forget-retain objectives: An efficient llm unlearning framework from logit difference. In *Annual Conference on Neural Information Processing Systems*, 2024b.
- Jia, J., Liu, J., Zhang, Y., Ram, P., Baracaldo, N., and Liu, S. Wagle: Strategic weight attribution for effective and modular unlearning in large language models. *arXiv preprint arXiv:2410.17509*, 2024a.

- Jia, J., Liu, J., Zhang, Y., Ram, P., Baracaldo, N., and Liu, S. Wagle: Strategic weight attribution for effective and modular unlearning in large language models. In *The Thirty-eighth Annual Conference on Neural Information Processing Systems*, 2024b.
- Khanov, M., Burapachee, J., and Li, Y. Args: Alignment as reward-guided search. *arXiv preprint arXiv:2402.01694*, 2024.
- Kim, M., Lee, H., Yoo, K. M., Park, J., Lee, H., and Jung, K. Critic-guided decoding for controlled text generation. In *Findings of the Association for Computational Linguistics: ACL 2023*, pp. 4598–4612, 2023.
- Kong, L., Wang, H., Mu, W., Du, Y., Zhuang, Y., Zhou, Y., Song, Y., Zhang, R., Wang, K., and Zhang, C. Aligning large language models with representation editing: A control perspective. *arXiv preprint arXiv:2406.05954*, 2024.
- Korbak, T., Shi, K., Chen, A., Bhalerao, R. V., Buckley, C., Phang, J., Bowman, S. R., and Perez, E. Pretraining language models with human preferences. In *International Conference on Machine Learning*, pp. 17506–17533. PMLR, 2023.
- Langley, P. Crafting papers on machine learning. In Langley, P. (ed.), *Proceedings of the 17th International Conference on Machine Learning (ICML 2000)*, pp. 1207–1216, Stanford, CA, 2000. Morgan Kaufmann.
- Li, J., Cheng, X., Zhao, W. X., Nie, J.-Y., and Wen, J.-R. Halueval: A large-scale hallucination evaluation benchmark for large language models. *arXiv preprint arXiv:2305.11747*, 2023.
- Li, N., Pan, A., Gopal, A., Yue, S., Berrios, D., Gatti, A., Li, J. D., Dombrowski, A.-K., Goel, S., Mukobi, G., et al. The wmdp benchmark: Measuring and reducing malicious use with unlearning. In *Forty-first International Conference on Machine Learning*, 2024.
- Liu, B., Liu, Q., and Stone, P. Continual learning and private unlearning. In *Conference on Lifelong Learning Agents*, pp. 243–254. PMLR, 2022.
- Liu, H., Simonyan, K., and Yang, Y. Darts: Differentiable architecture search. In *International Conference on Learning Representations*, 2019.
- Liu, J., Cohen, A., Pasunuru, R., Choi, Y., Hajishirzi, H., and Celikyilmaz, A. Making ppo even better: Value-guided monte-carlo tree search decoding. *arXiv preprint arXiv:2309.15028*, 2023.
- Liu, S., Yao, Y., Jia, J., Casper, S., Baracaldo, N., Hase, P., Yao, Y., Liu, C. Y., Xu, X., Li, H., et al. Rethinking machine unlearning for large language models. In *Annual Conference on Neural Information Processing Systems*, 2024a.
- Liu, T., Guo, S., Bianco, L., Calandriello, D., Berthet, Q., Llinares, F., Hoffmann, J., Dixon, L., Valko, M., and Blondel, M. Decoding-time realignment of language models. *arXiv preprint arXiv:2402.02992*, 2024b.
- Liu, Z., Dou, G., Tan, Z., Tian, Y., and Jiang, M. Towards safer large language models through machine unlearning. *arXiv preprint arXiv:2402.10058*, 2024c.
- Locatello, F., Tschannen, M., Rätsch, G., and Jaggi, M. Greedy algorithms for cone constrained optimization with convergence guarantees. *Advances in Neural Information Processing Systems*, 30, 2017.
- Loshchilov, I. Decoupled weight decay regularization. *arXiv preprint arXiv:1711.05101*, 2017.
- Lu, X., Welleck, S., Hessel, J., Jiang, L., Qin, L., West, P., Ammanabrolu, P., and Choi, Y. Quark: Controllable text generation with reinforced unlearning. *Advances in neural information processing systems*, 35:27591–27609, 2022.
- Maini, P., Feng, Z., Schwarzschild, A., Lipton, Z. C., and Kolter, J. Z. Tofu: A task of fictitious unlearning for llms. In *ICLR 2024 Workshop on Navigating and Addressing Data Problems for Foundation Models*, 2024.
- Mitchell, E., Rafailov, R., Sharma, A., Finn, C., and Manning, C. D. An emulator for fine-tuning large language models using small language models. In *The Twelfth International Conference on Learning Representations*, 2024.
- Mudgal, S., Lee, J., Ganapathy, H., Li, Y., Wang, T., Huang, Y., Chen, Z., Cheng, H.-T., Collins, M., Strohman, T., et al. Controlled decoding from language models. In *Forty-first International Conference on Machine Learning*, 2024.
- Nocedal, J. and Wright, S. J. Conjugate gradient methods. *Numerical optimization*, pp. 101–134, 2006.
- Ouyang, L., Wu, J., Jiang, X., Almeida, D., Wainwright, C., Mishkin, P., Zhang, C., Agarwal, S., Slama, K., Ray, A., et al. Training language models to follow instructions with human feedback. *Advances in neural information processing systems*, 35:27730–27744, 2022.
- Pedregosa, F. Hyperparameter optimization with approximate gradient. In *International conference on machine learning*, pp. 737–746. PMLR, 2016.

- Rafailov, R., Sharma, A., Mitchell, E., Manning, C. D., Ermon, S., and Finn, C. Direct preference optimization: Your language model is secretly a reward model. *Advances in Neural Information Processing Systems*, 36, 2024.
- Schulman, J., Wolski, F., Dhariwal, P., Radford, A., and Klimov, O. Proximal policy optimization algorithms. *arXiv preprint arXiv:1707.06347*, 2017.
- Shi, W., Ajith, A., Xia, M., Huang, Y., Liu, D., Blevins, T., Chen, D., and Zettlemoyer, L. Detecting pretraining data from large language models. *arXiv preprint arXiv:2310.16789*, 2023.
- Stiennon, N., Ouyang, L., Wu, J., Ziegler, D., Lowe, R., Voss, C., Radford, A., Amodei, D., and Christiano, P. F. Learning to summarize with human feedback. *Advances in Neural Information Processing Systems*, 33: 3008–3021, 2020.
- Su, Y., Lan, T., Wang, Y., Yogatama, D., Kong, L., and Collier, N. A contrastive framework for neural text generation. *Advances in Neural Information Processing Systems*, 35:21548–21561, 2022.
- Tian, B., Liang, X., Cheng, S., Liu, Q., Wang, M., Sui, D., Chen, X., Chen, H., and Zhang, N. To forget or not? towards practical knowledge unlearning for large language models. In *Findings of the Association for Computational Linguistics: EMNLP 2024*, pp. 1524–1537, 2024.
- Touvron, H., Martin, L., Stone, K., Albert, P., Almahairi, A., Babaei, Y., Bashlykov, N., Batra, S., Bhargava, P., Bhosale, S., et al. Llama 2: Open foundation and fine-tuned chat models. *arXiv preprint arXiv:2307.09288*, 2023.
- Tunstall, L., Beeching, E., Lambert, N., Rajani, N., Rasul, K., Belkada, Y., Huang, S., von Werra, L., Fourier, C., Habib, N., et al. Zephyr: Direct distillation of lm alignment. *arXiv preprint arXiv:2310.16944*, 2023.
- Wan, Z., Feng, X., Wen, M., McAleer, S. M., Wen, Y., Zhang, W., and Wang, J. Alphazero-like tree-search can guide large language model decoding and training. In *Forty-first International Conference on Machine Learning*, 2024.
- Wang, L., Chen, T., Yuan, W., Zeng, X., Wong, K.-F., and Yin, H. Kga: A general machine unlearning framework based on knowledge gap alignment. In *Proceedings of the 61st Annual Meeting of the Association for Computational Linguistics (Volume 1: Long Papers)*, pp. 13264–13276, 2023.
- Wang, Y., Wei, J., Liu, C. Y., Pang, J., Liu, Q., Shah, A. P., Bao, Y., Liu, Y., and Wei, W. Llm unlearning via loss adjustment with only forget data. *arXiv preprint arXiv:2410.11143*, 2024.
- Wu, Y., Sun, Z., Yuan, H., Ji, K., Yang, Y., and Gu, Q. Self-play preference optimization for language model alignment. *arXiv preprint arXiv:2405.00675*, 2024.
- Xiao, T., Yuan, Y., Zhu, H., Li, M., and Honavar, V. G. Cal-dpo: Calibrated direct preference optimization for language model alignment. *arXiv preprint arXiv:2412.14516*, 2024.
- Xu, Z., Huang, R., Chen, C., and Wang, X. Uncovering safety risks of large language models through concept activation vector. In *The Thirty-eighth Annual Conference on Neural Information Processing Systems*, 2024.
- Yao, Y., Xu, X., and Liu, Y. Large language model unlearning. In *Annual Conference on Neural Information Processing Systems*, 2024.
- Zhang, R., Lin, L., Bai, Y., and Mei, S. Negative preference optimization: From catastrophic collapse to effective unlearning. *arXiv preprint arXiv:2404.05868*, 2024.
- Zhou, Z., Liu, Z., Liu, J., Dong, Z., Yang, C., and Qiao, Y. Weak-to-strong search: Align large language models via searching over small language models. *arXiv preprint arXiv:2405.19262*, 2024.
- Ziegler, D. M., Stiennon, N., Wu, J., Brown, T. B., Radford, A., Amodei, D., Christiano, P., and Irving, G. Fine-tuning language models from human preferences. *arXiv preprint arXiv:1909.08593*, 2019.
- Zou, A., Wang, Z., Carlini, N., Nasr, M., Kolter, J. Z., and Fredrikson, M. Universal and transferable adversarial attacks on aligned language models. *arXiv preprint arXiv:2307.15043*, 2023.

A. Discussion on the Definition of Unlearning in LLMs

In this section, we review and summarize the definitions of existing unlearning methods for LLMs and attempt to incorporate these methods into a unified theoretical framework. Assume the training dataset is denoted as $\mathcal{D}_t = \mathcal{D}_f \cup \mathcal{D}_r$, where \mathcal{D}_f represents the set of samples to be unlearned, and \mathcal{D}_r represents the remaining samples. The core objective of LLM unlearning is to remove the knowledge learned from \mathcal{D}_f while preserving the model’s other capabilities as much as possible. To achieve this goal, existing methods can be broadly categorized into two main classes: (i) gradient-based methods and (ii) preference optimization-based methods.

Gradient-based methods. Gradient-based methods include gradient ascent and its various extensions. Below, we will review the definitions of these methods sequentially.

Gradient ascent. Gradient ascent (Jang et al., 2023; Feng et al., 2024) is a traditional and straightforward baseline method that removes the model’s memory of the samples in \mathcal{D}_f by maximizing the loss on \mathcal{D}_f , effectively reversing the gradient descent process. It is defined as:

$$\mathcal{L}_{\text{GA}} = \underbrace{\frac{1}{|\mathcal{D}_f|} \sum_{i=1}^{|\mathcal{D}_f|} \sum_{t=1}^{n_i} \log p(x_t | \mathbf{x}_{<t}; \boldsymbol{\theta})}_{\mathcal{L}_{\text{forget}}(\mathcal{D}_f; \boldsymbol{\theta})},$$

where n_i denotes the number of tokens in the sample \mathbf{x}^i , and $\boldsymbol{\theta}$ represents the parameters of the model.

Variants of gradient ascent. However, naive gradient ascent significantly degrades the model’s other capabilities. To address this issue, recent studies (Wang et al., 2023; Li et al., 2024; Maini et al., 2024; Ji et al., 2024b; Jia et al., 2024b; Liu et al., 2024a; Wang et al., 2024) have introduced various regularization terms, primarily including loss-based regularization and divergence-based regularization, as described below:

- **Loss-based regularization.** Loss-based regularization (Li et al., 2024; Maini et al., 2024; Jia et al., 2024b) maintains the model’s other capabilities by sampling a dataset \mathcal{D}'_r that shares the same distribution as \mathcal{D}_r and minimizing the model’s loss on \mathcal{D}'_r . The formal expression is:

$$\mathcal{L}_{\text{GA+LR}} = \underbrace{\mathcal{L}_{\text{GA}}}_{\mathcal{L}_{\text{forget}}(\mathcal{D}_f; \boldsymbol{\theta})} - \lambda \underbrace{\frac{1}{|\mathcal{D}'_r|} \sum_{i=1}^{|\mathcal{D}'_r|} \sum_{t=1}^{n_i} \log p(x_t | \mathbf{x}_{<t}; \boldsymbol{\theta})}_{\mathcal{L}_{\text{reg}}(\boldsymbol{\theta})}.$$

- **Divergence-based regularization.** Similar to loss-based regularization, divergence-based regularization (Wang et al., 2023; Tian et al., 2024; Maini et al., 2024; Ji et al., 2024b; Wang et al., 2024) preserves model performance by constraining the output distribution of the model on a dataset \mathcal{D}'_r . Specifically, this method minimizes the distributional distance $\text{Dis}(\cdot || \cdot)$ between the output distribution of the unlearned model on \mathcal{D}'_r and that of the original model on \mathcal{D}'_r . Depending on the metric used to measure the distributional distance, this method can further be categorized into regularizations based on KL divergence (Wang et al., 2023; Maini et al., 2024) and f-divergence (Wang et al., 2024). The formal definition is:

$$\mathcal{L}_{\text{GA+DR}} = \underbrace{\mathcal{L}_{\text{GA}}}_{\mathcal{L}_{\text{forget}}(\mathcal{D}_f; \boldsymbol{\theta})} + \lambda \underbrace{\frac{1}{|\mathcal{D}'_r|} \sum_{i=1}^{|\mathcal{D}'_r|} \sum_{t=1}^{n_i} \text{Dis}(P(\cdot | \mathbf{x}_{<t}; \boldsymbol{\theta}) || P(\cdot | \mathbf{x}_{<t}; \boldsymbol{\theta}^*))}_{\mathcal{L}_{\text{reg}}(\boldsymbol{\theta})}.$$

Both loss regularization and divergence regularization can essentially be regarded as forms of parameter regularization, which constrain the norm of the difference between model parameters before and after unlearning to be less than a threshold δ . By restricting the parameter changes within a δ -norm ball, this technique ensures the preservation of the model’s other capabilities. However, parameter regularization is difficult to handle directly as a constraint, so its relaxed form is often utilized and incorporated into the objective function instead. Formally, this can be expressed as:

$$\mathcal{L}_{\text{GA+PR}} = \underbrace{\mathcal{L}_{\text{GA}}}_{\mathcal{L}_{\text{forget}}(\mathcal{D}_f; \boldsymbol{\theta})} + \lambda \underbrace{\|\boldsymbol{\theta} - \boldsymbol{\theta}^*\|_p^2}_{\mathcal{L}_{\text{reg}}(\boldsymbol{\theta})}.$$

In addition, while several recent methods (i.e., Mismatch and LLMU) (Yao et al., 2024) differ in their definitions of unlearning objectives, they are fundamentally variants of gradient ascent methods. These methods further refine gradient ascent by extending the formulation of unlearning objectives, constructing a random combination of text sequences Y_{ran} . Specifically, their definitions are given as:

$$\begin{aligned}\mathcal{L}_{\text{MIS}} &= \underbrace{-\frac{1}{|\mathcal{D}_f|} \sum_{i=1}^{|\mathcal{D}_f|} \sum_{t=1}^{n_i} \frac{1}{|Y_{\text{ran}}|} \sum_{j=1}^{|Y_{\text{ran}}|} \log p(y_{\text{ran}}^j | \mathbf{x}_{<t}; \boldsymbol{\theta})}_{\mathcal{L}_{\text{forget}}(\mathcal{D}_f; \boldsymbol{\theta})} - \lambda \underbrace{\frac{1}{|\mathcal{D}'_r|} \sum_{i=1}^{|\mathcal{D}'_r|} \sum_{t=1}^{n_i} \log p(x_t | \mathbf{x}_{<t}; \boldsymbol{\theta})}_{\mathcal{L}_{\text{reg}}(\boldsymbol{\theta})}. \\ \mathcal{L}_{\text{LLMU}} &= \underbrace{\mathcal{L}_{\text{GA}} - \frac{1}{|\mathcal{D}_f|} \sum_{i=1}^{|\mathcal{D}_f|} \sum_{t=1}^{n_i} \frac{1}{|Y_{\text{ran}}|} \sum_{j=1}^{|Y_{\text{ran}}|} \log p(y_{\text{ran}}^j | \mathbf{x}_{<t}; \boldsymbol{\theta})}_{\mathcal{L}_{\text{forget}}(\mathcal{D}_f; \boldsymbol{\theta})} + \lambda \underbrace{\frac{1}{|\mathcal{D}'_r|} \sum_{i=1}^{|\mathcal{D}'_r|} \sum_{t=1}^{n_i} \text{Dis}(P(\cdot | \mathbf{x}_{<t}; \boldsymbol{\theta}) || P(\cdot | \mathbf{x}_{<t}; \boldsymbol{\theta}^*))}_{\mathcal{L}_{\text{reg}}(\boldsymbol{\theta})}.\end{aligned}$$

Preference optimization-based methods. Preference optimization-based unlearning methods for LLMs primarily include DPO (Lu et al., 2022; Maini et al., 2024; Dige et al., 2024) and its variants, as well as Negative Preference Optimization (NPO) (Zhang et al., 2024; Fan et al., 2024). These methods achieve unlearning by constructing additional preference data pairs and leveraging existing preference optimization algorithms to guide the model.

DPO method. The DPO method constructs preference data pairs based on the unlearning sample set (Lu et al., 2022; Maini et al., 2024; Dige et al., 2024). For example, given a sample \mathbf{x}^i containing n_i combinations, for any combination pair $(\mathbf{x}_{<t}^i, x_t)$, where x_t is the truthful response, DPO sets x'_t as "refuse to answer" and treats it as the preferred response. By optimizing this preference pair, DPO employs preference optimization algorithms to achieve unlearning. It is formally defined as:

$$\mathcal{L}_{\text{DPO}} = -\frac{2}{\beta} \mathbb{E}_{\mathbf{x}^i \in \mathcal{D}_f} \left[\log \sigma \left(\underbrace{-\beta \sum_{i=1}^{n_i} \log p(x_t | \mathbf{x}_{<t}; \boldsymbol{\theta})}_{\mathcal{L}_{\text{forget}}(\mathcal{D}_f; \boldsymbol{\theta})} + \underbrace{\beta \sum_{i=1}^{n_i} \log p(x'_t | \mathbf{x}_{<t}; \boldsymbol{\theta}) - M_{\text{ref}}}_{\mathcal{L}_{\text{reg}}(\boldsymbol{\theta})} \right) \right].$$

NPO method. The NPO method directly treats the unlearning samples as negative samples and penalizes the model's responses on the unlearning set \mathcal{D}_f (Zhang et al., 2024; Fan et al., 2024). The formal definition is:

$$\mathcal{L}_{\text{NPO}} = -\frac{2}{\beta} \mathbb{E}_{\mathbf{x}^i \in \mathcal{D}_f} \left[\log \sigma \left(\underbrace{-\beta P(x_t | \mathbf{x}_{<t}^i; \boldsymbol{\theta}^*)}_{\mathcal{L}_{\text{forget}}(\text{forget}; \boldsymbol{\theta})} + \underbrace{\beta \log P(x_t | \mathbf{x}_{<t}^i; \boldsymbol{\theta})}_{\mathcal{L}_{\text{reg}}(\boldsymbol{\theta})} \right) \right]$$

In summary, both gradient-based methods and preference optimization-based methods can be viewed as combinations of unlearning loss and regularization loss.

B. Theoretical Analysis

B.1. Proof of Proposition 4.2

To analyze the variation of $\mathcal{J}(\boldsymbol{\theta}^*(\epsilon))$, we perform a Taylor expansion of Eq. (6) around $\epsilon = 0$. Here, since we are more concerned with the description of the magnitude of the effect rather than the exact values, we expand it only to the first-order term, yielding:

$$\mathcal{J}(\boldsymbol{\theta}^*(\epsilon)) \approx \mathcal{J}(\boldsymbol{\theta}^*(0)) + \epsilon \frac{\partial \mathcal{J}(\boldsymbol{\theta}^*(\epsilon))}{\partial \epsilon} \Big|_{\epsilon=0},$$

where $\mathcal{J}(\boldsymbol{\theta}^*(0))$ represents the preference alignment performance of the model at $\epsilon = 0$ (i.e., without unlearning), while $\frac{\partial \mathcal{J}(\boldsymbol{\theta}^*(\epsilon))}{\partial \epsilon}$ denotes the rate of change in the PA performance w.r.t. the unlearning weight control parameter ϵ . According to the chain rule, the partial derivative can be decomposed as:

$$\frac{\partial \mathcal{J}(\boldsymbol{\theta}^*(\epsilon))}{\partial \epsilon} = \nabla_{\boldsymbol{\theta}} \mathcal{J}(\boldsymbol{\theta}^*(\epsilon))^{\top} \frac{\partial \boldsymbol{\theta}^*(\epsilon)}{\partial \epsilon}.$$

Since the optimal solution $\theta^*(\epsilon)$ of the lower-level problem satisfies the first-order optimality condition:

$$\nabla_{\theta} (\epsilon \mathcal{L}_{\text{forget}}(\mathbf{x}; \theta) + \mathcal{L}_{\text{reg}}(\theta))|_{\theta=\theta^*(\epsilon)} = 0.$$

By differentiating the above optimality condition w.r.t ϵ , we obtain:

$$\epsilon \nabla_{\theta}^2 \mathcal{L}_{\text{forget}}(\mathbf{x}; \theta^*(\epsilon)) \frac{\partial \theta^*(\epsilon)}{\partial \epsilon} + \nabla_{\theta} \mathcal{L}_{\text{forget}}(\mathbf{x}; \theta^*(\epsilon)) + \nabla_{\theta}^2 \mathcal{L}_{\text{reg}}(\theta^*(\epsilon)) \frac{\partial \theta^*(\epsilon)}{\partial \epsilon} = 0.$$

Substituting $\mathcal{L}_{\text{reg}}(\theta) = \|\theta - \theta^*\|^2$, we have:

$$\nabla_{\theta} \mathcal{L}_{\text{reg}}(\theta^*(\epsilon)) = 2(\theta^*(\epsilon) - \theta^*), \quad \nabla_{\theta}^2 \mathcal{L}_{\text{reg}}(\theta^*(\epsilon)) = 2I.$$

Therefore, the implicit gradient formula is given by:

$$\frac{\partial \theta^*(\epsilon)}{\partial \epsilon} = - [\epsilon \nabla_{\theta}^2 \mathcal{L}_{\text{forget}}(\mathbf{x}; \theta^*(\epsilon)) + 2I]^{-1} \nabla_{\theta} \mathcal{L}_{\text{forget}}(\mathbf{x}; \theta^*(\epsilon)).$$

When $\epsilon = 0$, the formula simplifies to:

$$\frac{\partial \theta^*(\epsilon)}{\partial \epsilon}|_{\epsilon=0} = - [2I]^{-1} \nabla_{\theta} \mathcal{L}_{\text{forget}}(\mathbf{x}; \theta^*(0)) = -\frac{1}{2} \nabla_{\theta} \mathcal{L}_{\text{forget}}(\mathbf{x}; \theta^*).$$

Substituting $\frac{\partial \theta^*(\epsilon)}{\partial \epsilon}$ into the chain rule formula:

$$\frac{\partial \mathcal{J}(\theta^*(\epsilon))}{\partial \epsilon}|_{\epsilon=0} = \nabla_{\theta} \mathcal{J}(\theta^*)^{\top} \left(-\frac{1}{2} \nabla_{\theta} \mathcal{L}_{\text{forget}}(\mathbf{x}; \theta^*) \right).$$

Therefore, the variation in preference alignment performance is:

$$\mathcal{J}(\theta^*(\epsilon)) - \mathcal{J}(\theta^*(0)) \approx -\frac{\epsilon}{2} \nabla_{\theta} \mathcal{J}(\theta^*)^{\top} \nabla_{\theta} \mathcal{L}_{\text{forget}}(\mathbf{x}; \theta^*).$$

B.2. Derivation of Marginal Gain

To optimize the outer problem, we need to compute the gradient of the objective function w.r.t. the weight vector ω :

$$\begin{aligned} \nabla_{\omega} g(\omega) &= -\nabla_{\omega} \mathcal{J}(\theta^*(\omega)) + \beta \sum_{i=1}^n \sqrt{\omega} \\ &= -\frac{\partial \mathcal{J}(\theta^*(\omega))}{\partial \theta} \frac{\partial \theta^*(\omega)}{\partial \omega} + \left[\frac{\beta}{2\sqrt{\omega_1}}, \frac{\beta}{2\sqrt{\omega_2}}, \dots, \frac{\beta}{2\sqrt{\omega_n}} \right]^{\top}. \end{aligned} \quad (13)$$

Since the solution of the inner optimization problem $\theta^*(\omega)$ satisfies the first-order necessary condition:

$$\nabla_{\theta} f(\theta^*(\omega), \omega) = 0,$$

which is equivalent to

$$\nabla_{\theta} \left(\sum_{i=1}^n \omega_i \ell_i(\theta^*(\omega)) + \lambda \|\theta^*(\omega) - \theta^*\|^2 \right) = 0.$$

Taking the derivative w.r.t. ω , and using the implicit function theorem, we obtain:

$$\begin{aligned} \frac{\partial \theta^*(\omega)}{\partial \omega} &= - \left(\frac{\partial^2 f}{\partial \theta^2} \right)^{-1} \frac{\partial^2 f}{\partial \theta \partial \omega} \\ &= - \left(\frac{\partial^2 f}{\partial \theta^2} \right)^{-1} \frac{\partial}{\partial \omega} \left[\sum_{i=1}^n \omega_i \frac{\partial \ell_i(\theta)}{\partial \theta} + 2\lambda(\theta - \theta^*) \right], \end{aligned} \quad (14)$$

where $\frac{\partial^2 f}{\partial \theta^2} = \sum_{i=1}^n \omega_{S_{t-1},i}^* \nabla_{\theta}^2 \ell_i(\theta^*(\omega)) + 2\lambda I$ denotes the Hessian matrix of the inner optimization problem. Substituting Eq. (14) into Eq. (13):

$$\nabla_{\omega} g(\omega) = \frac{\partial \mathcal{J}(\theta^*(\omega))}{\partial \theta} \left(\frac{\partial^2 f}{\partial \theta^2} \right)^{-1} \frac{\partial}{\partial \omega} \left[\sum_{i=1}^n \omega_i \frac{\partial \ell_i(\theta)}{\partial \theta} + 2\lambda(\theta - \theta^*) \right] + \left[\frac{\beta}{2\sqrt{\omega_1}}, \frac{\beta}{2\sqrt{\omega_2}}, \dots, \frac{\beta}{2\sqrt{\omega_n}} \right]^{\top}.$$

Now, consider the contribution of the k -th component of the weight vector ω to $g(\omega)$, i.e., computing $\frac{\partial g(\omega)}{\partial \omega_k}$. Since only when $i = k$, the term corresponding to ω_k contributes, we derive:

$$\Delta g(k) = \frac{\partial g(\omega)}{\partial \omega_k} = \nabla_{\theta} \mathcal{J}(\theta^*(\omega)) \left(\frac{\partial^2 f}{\partial \theta^2} \right)^{-1} \nabla_{\theta} \ell_k(\theta^*(\omega)) + \frac{\beta}{2} \omega_k^{-\frac{1}{2}}.$$

B.3. Derivation of Set Size

The suboptimality bound provided by Theorem 4.3 is given as:

$$g(\omega_{S_t}^*) - g(\omega^*) \leq \frac{8L + 4\varepsilon_1}{t + 3}.$$

To satisfy the suboptimality error constraint, i.e., $g(\omega_{S_t}^*) - g(\omega^*) \leq \varepsilon$, it suffices to ensure that the right-hand side of the suboptimality bound is less than or equal to ε , which gives: $\frac{8L + 4\varepsilon_1}{t + 3} \leq \varepsilon$.

By moving $t + 3$ to the right-hand side and expanding the terms on the right, we obtain: $\varepsilon t \geq 8L + 4\varepsilon_1 - 3\varepsilon$. Neglecting -3ε (as its impact diminishes with increasing t), the expression is further simplified to: $\varepsilon t \geq 8L + 4\varepsilon_1$.

Moving ε to the right-hand side yields: $t \geq \frac{8L + 4\varepsilon_1}{\varepsilon}$. This indicates that, to satisfy the suboptimality error constraint $g(\omega_{S_t}^*) - g(\omega^*) \leq \varepsilon$, the number of iterations t must be at least: $t = \mathcal{O}(\frac{L + \varepsilon_1}{\varepsilon})$.

C. Additional Experimental Details

C.1. Dataset Configurations

The detailed partitioning for each dataset is as follows:

- For the PKU SafeRLHF, samples of type harmful or risk-inducing across at least one of the 19 harm categories are defined as negative examples.
- For the UltraFeedback Binarized, samples of type low ratings in instruction following, truthfulness, honesty, or helpfulness annotations are considered negative examples.
- For the HaluEval, samples meeting the unverifiable, non-factual, or irrelevant hallucination annotations condition are categorized as negative examples.

C.2. Evaluation Configurations

In this section, we provide a detailed explanation of each evaluation metric.

For the performance of PA, we utilize the following four evaluation metrics:

- **Reward-value** (Chakraborty et al., 2024; Yao et al., 2024). Reward-value assesses the quality of the model’s outputs based on reward scores assigned by the reward model. Higher values for these two metrics indicate better PA performance of the model after unlearning.
- **ASR** (Xu et al., 2024). ASR measures the model’s tendency to generate potentially harmful content. In our experiments, ASR is further divided into four sub-dimensions (Xu et al., 2024; Zou et al., 2023): ASR-keyword, ASR-answer, ASR-useful, and ASR-summary. Smaller values for these metrics indicate better PA performance of the model after unlearning.

- **Coherence** (Chakraborty et al., 2024; Khanov et al., 2024; Kong et al., 2024). Coherence is evaluated by calculating the cosine similarity between the SimCSE (Su et al., 2022) embeddings of each prompt and its generated response, assessing their semantic proximity (Chakraborty et al., 2024). Higher coherence indicates better PA performance.
- **Win-rate** (Xiao et al., 2024; Rafailov et al., 2024). Win-rate measures the proportion of instances where the model’s outputs are preferred over those of the baseline model (GPT-4).
- **Hallucination-rate** (Yao et al., 2024). Hallucination-rate measures the frequency of false or factually incorrect information in the outputs. A lower hallucination-rate indicates better PA performance.

For the performance of unlearning, we utilize the following three evaluation metrics:

- **Membership Inference Attack (MIA)** (Jia et al., 2024a). We employ the Min- k % Prob (Shi et al., 2023) method to calculate the likelihood of a given text belonging to the training data. The specific metric used is the area under the ROC curve (AUC). A higher AUC value indicates that the model is better at distinguishing between training and non-training data, thereby demonstrating greater unlearning effectiveness.
- **Perplexity (PPL)** (Yao et al., 2024; Doshi & Stickland, 2024). Lower PPL values indicate higher quality of the generated text, with outputs being more fluent and consistent with natural language expression norms.

D. Additional Experiments

We validated the effectiveness of U2A on the UltraFeedback Binarized and HaluEval datasets. The experimental results are shown in the table below.

Table 3. Comparison of the U2A framework with the current PA and unlearning baseline methods on the UltraFeedback Binarized dataset. Optimal results are highlighted in **bold**.

Models	Methods	PA Performance			MU Performance	
		Length-control Win Rate (\uparrow)	Win Rate vs. GPT-4 (\uparrow)	Coherence (\uparrow)	MIA (\uparrow)	PPL (\downarrow)
Llama-2-7B-Chat	Original Retrain	0.0818	0.0534	0.7519	0.5287	9.3005
		0.0770	0.0309	0.7571	0.5058	9.3588
	PPO DPO	0.0916	0.0586	0.7643	0.5618	11.3477
		0.0886	0.0620	0.7618	0.5410	10.1612
	GA GradDiff NPO	0.0792	0.0523	0.7516	0.5337	8.4104
		0.0822	0.0653	0.7632	0.5735	9.0017
		0.0808	0.0581	0.7574	0.5288	10.1905
	GA + U2A GradDiff + U2A NPO + U2A	0.0985	0.0697	0.7632	0.5244	8.3768
		0.1002	0.0711	0.7678	0.5845	8.8979
		0.0992	0.0724	0.7603	0.5505	9.4683
Llama-3.1-8B-Instruct	Original Retrain	0.2330	0.2281	0.7508	0.5358	2.6358
		0.2411	0.2363	0.7521	0.5401	2.6408
	PPO DPO	0.2453	0.2325	0.7588	0.5327	2.8744
		0.2597	0.2447	0.7603	0.5358	2.9620
	GA GradDiff NPO	0.2374	0.2338	0.7498	0.5313	2.6286
		0.2493	0.2456	0.7513	0.5364	2.6357
		0.2042	0.1751	0.7492	0.3812	3.1217
	GA + U2A GradDiff + U2A NPO + U2A	0.2522	0.2579	0.7612	0.5596	2.3941
		0.2515	0.2585	0.7572	0.5458	1.6617
		0.2391	0.2293	0.7601	0.5192	2.9896

Table 4. Comparison of the U2A framework with the current PA and unlearning baseline methods on the HaluEval dataset. Optimal results are highlighted in **bold**.

Models	Methods	PA Performance			MU Performance	
		Hallucination Rate			MIA (\uparrow)	PPL (\downarrow)
		F1 (\downarrow)	Precision (\downarrow)	Recall (\downarrow)		
Llama-2-7B-Chat	Original	65.05	72.50	53.70	0.3945	118.0564
		Retrain	52.45	59.45	0.4006	98.8235
	PPO	55.35	61.80	44.85	0.3489	140.6214
		DPO	54.40	61.40	0.3985	116.9673
	GA	60.80	61.75	49.40	0.3938	70.1965
		GradDiff	59.34	62.45	0.3929	72.5341
		NPO	65.15	61.95	0.3988	104.3602
	GA + U2A	50.45	60.75	41.35	0.4061	66.2969
		GradDiff + U2A	49.90	60.65	0.4165	64.1484
		NPO + U2A	48.45	58.70	40.05	67.8125
Llama-3.1-8B-Instruct	Original	57.05	65.45	46.00	0.3903	7.1921
		Retrain	52.90	58.20	0.3978	7.5665
	PPO	55.85	62.95	45.70	0.3908	6.8384
		DPO	56.55	64.80	0.4083	7.1947
	GA	53.40	65.20	44.60	0.4345	8.9799
		GradDiff	58.35	70.55	0.4565	7.4564
		NPO	58.05	65.35	0.3908	12.4844
	GA + U2A	50.65	58.10	40.95	0.4422	6.7682
		GradDiff + U2A	49.75	56.35	0.4571	7.8976
		NPO + U2A	48.15	55.40	0.4220	9.9792